Analytical Design of a Wide Class of Controllers with Two Tunable Parameters Based on H_∞ Specifications

Michal Brabec[1], Miloš Schlegel[2]

[1] *brabecm@ntis.zcu.cz - Department of Cybernetics, Faculty of Applied Sciences, University of West Bohemia, Pilsen, Czechia*
[2] *schlegel@ntis.zcu.cz - NTIS Research Center, Faculty of Applied Sciences, University of West Bohemia, Pilsen, Czechia*

This is the accepted version of the article. The final published version is available from IEEE Xplore at: https://ieeexplore.ieee.org/document/10217459.

Full citation: M. Brabec and M. Schlegel, "*Analytical Design of a Wide Class of Controllers with Two Tunable Parameters Based on H_∞ Specifications,*" 24th International Conference on Process Control (PC), Strbske Pleso, Slovakia, 2023, pp. 221-226, doi: 10.1109/PC58330.2023.10217459.

Abstract
First, the paper introduces a specific class of controllers with two tunable parameters called *affine controllers*, which includes almost all controllers with a fixed structure commonly used in industrial practice, including PI(D) controllers. The main result of this paper presents a new analytical method for the design of the H_∞ affine controller based on a description of the boundary of the H_∞ region in the parametric plane of the controller. A user-friendly interactive implementation of this method, supporting multiple system models, is available at *www.pidlab.com*. The use of this tool is also illustrated by an example.

Keywords
fixed order controller, H_∞ affine controller, parametric plane, PID Hinf Designer

Contents

1. Introduction

Robust controller design plays a crucial role in various industrial applications, but finding a good controller setting that meets complex engineering design requirements is a challenging problem.

The robust control design techniques, which generally use optimization in the frequency domain with utilization H_2 and H_∞ norms [17], provides an accurate formulation of the problem and its solution. However, the synthesized controller is not very applicable in practice [2]. Computation via algebraic Riccati equations (AREs) or linear matrix inequalities (LMIs) may result in general high-order controllers compared to the plant. Moreover, the offered solutions are quite fragile. Small perturbations of the controller coefficients destabilize the controlled system [10].

Thus, the academic community tried to circumvent the mentioned shortcomings by finding a method using the direct design of fixed-order controllers, which are the most widely used in the industry. However, this is a complex optimization problem because it is well known that the design of a fixed-order controller based on H_∞ specifications is a non-convex NP-hard problem, and all solutions to this problem are based on certain approximations [2]. However, if we focus on the case where the desired controller has only two or three adjustable parameters, it is possible to use the parametric space approach. The solution to the design problem can then be expressed by a region in the parametric plane of the controller. Points of this region represent all stabilization controllers or controllers that meet specified design requirements. These requirements are most often given in the form of H_∞ specifications that reflect the essence of the real problems in the field of process control.

There are different approaches to finding such regions ([3, 14, 15]), mainly focused on PI or PID controllers. In [9], is introduced a method for characterizing all stabilizing PID controllers, based on the generalized Hermite-Biehler theorem. All admissible H_∞ PID controllers are then determined by a linear programming-based algorithm. An alternative path was taken by [1, 4]. The fundamental concept of this approach is reducing robust multi-objective feedback design to quantifier elimination problems, which further enables a resolution of many control synthesis problems that are difficult to solve by classical numerical methods. A non-convex optimization method is presented in [18]. The region in the parametric plane is obtained based on the parameterization of all stabilizing PI controllers and envelop of the set of ellipses. The D-decomposition paradigm defines the admissible region in [6–8, 13].

This paper describes a new analytical method for the design of the H_∞ affine controller. The used affine structure can describe a wide class of controllers with two tunable and any number of fixed parameters, useful in various industrial applications. The presented method is based on an analytical, computational procedure for translating a wide range of H_∞ design specifications to the boundary of the H_∞ region. By the used approach of H_∞ region boundary, this work follows on [13]. Through the intersection of H_∞ regions in the parametric plane is possible to be implemented both single and multiple system models design and, at the same time, demand fulfillment of several H_∞ limitations. There are no important restrictions on the systems themselves. They can be unstable, non-minimum phase, oscillating systems, or systems with time delays (using the Pade approximation).

The paper is organized into five sections. Section II presents the basic assumptions and a brief theoretical basis of the research problem. Section III is devoted to the formulation of the analytical design method. Section IV contains basic information about the PID Hinf Designer software and one practical example. The paper's conclusion is in Section V. An appendix is attached after it.

2. Preliminaries And Problem Statements

2.1 Control Loop

Consider a closed-loop control system shown in Fig. 1, where $P(s)$ is a rational transfer function describing a LTI SISO plant of arbitrary order.

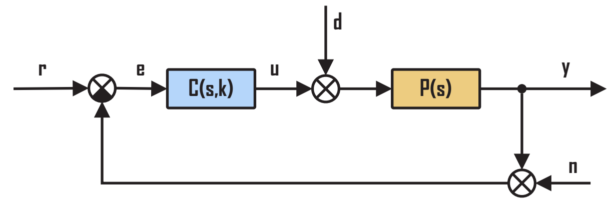

Figure 1. A standard feedback system

The fixed structure controller $C(s,\mathbf{k})$ is assumed in the form of affine function

$$C(s,\mathbf{k}) \triangleq k_q Q(s) + k_r R(s) + F(s), \tag{1}$$

where $Q(s)$, $R(s)$, and $F(s)$ are arbitrary rational transfer functions. The transfer function of the controller (1) is affinely dependent on the vector parameter $\mathbf{k} \triangleq [k_r, k_q]^T \in \mathbb{R}^2$. The control loop in Fig. 1 has the following sensitivity functions:

$$T(s,\mathbf{k}) = \frac{C(s,\mathbf{k})P(s)}{1 + C(s,\mathbf{k})P(s)}, \tag{2}$$

$$S(s,\mathbf{k}) = \frac{1}{1 + C(s,\mathbf{k})P(s)}, \tag{3}$$

$$S_p(s,\mathbf{k}) = \frac{P(s)}{1 + C(s,\mathbf{k})P(s)}, \tag{4}$$

$$S_c(s,\mathbf{k}) = \frac{C(s,\mathbf{k})}{1 + C(s,\mathbf{k})P(s)}. \tag{5}$$

2.2 Selection of $Q(s)$, $R(s)$, and $F(s)$ transfer functions

The choice of transfer functions $Q(s)$, $R(s)$, and $F(s)$ of the controller is part of the design problem and can be done based on different requirements:

- The structure of the proposed controller is given. In such a case, it is necessary to convert it into the form of the transfer function (1) and thus obtain the transfer functions $Q(s)$, $R(s)$, and $F(s)$. If the controller has more than two design parameters, the others must be fixed.

- We choose the transfer functions $Q(s)$, $R(s)$, and $F(s)$ based on the principle of the internal model in order to achieve tracking of the reference value or suppression of the disturbance of the given type, respectively.

- Consider the case where it is requested to enhance the existing controller $C_0(s)$. In such a case, $F(s) = C_0(s)$ can be set. $Q(s)$ and $R(s)$ can then be chosen appropriately to achieve an improvement in the closed-loop performance. This procedure can be iteratively repeated to increase the order of the controller. We can describe it in a simplified way by the following steps:

Step 1: A design of

$$C_0(s, \mathbf{k}_0) = k_{q0}Q_0(s) + k_{r0}R_0(s) + F_0(s)$$

$$\vdots$$

Step i: A design of

$$C_i(s, \mathbf{k}_i) = k_{qi}Q_i(s) + k_{ri}R_i(s) + C_{i-1}(s, \mathbf{k}_{i-1})$$

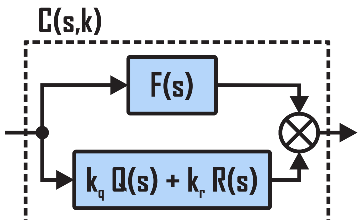

Figure 2. Affine controller structure

By a suitable choice of basis functions, it is possible to obtain almost all common controllers with a fixed structure used in practical applications:

- **PI controller**: A proportional–integral controller

$$C_{PI}(s) = k \cdot \left(1 + \frac{1}{T_i s}\right) = k_q + k_r \frac{1}{s} \tag{6}$$

is probably the most used control algorithm in process control and can be obtained as

$$Q(s) = 1, \quad R(s) = \frac{1}{s}, \quad F(s) = 0. \tag{7}$$

- **PD controller**: The primary benefit of a proportional derivative controller

$$C_{PD}(s) = k \cdot \left(1 + \frac{Tds}{\tau s + 1}\right) = k_q + k_r \frac{s}{\tau s + 1} \tag{8}$$

is the ability to damp oscillations in the system and can be obtained as

$$Q(s) = 1, \quad R(s) = \frac{s}{\tau s + 1}, \quad F(s) = 0. \tag{9}$$

- **PID controller**: A proportional integral derivative controller

$$\begin{aligned} C_{PID}(s) &= k \cdot \left(1 + \frac{1}{T_i s} + \frac{Tds}{\tau s + 1}\right) \\ &= k_p + k_i \frac{1}{s} + k_d \frac{s}{\tau s + 1} \end{aligned} \tag{10}$$

already contains more unknown variables, and thus there are several feasible settings. One possible approach is H_∞ region design in k_i/k_d plane with fixed k_p value [9].

$$Q(s) = \frac{s}{\tau s + 1}, \quad R(s) = \frac{1}{s}, \quad F(s) = k_p. \tag{11}$$

- **PR controller**: A proportional resonant controller

$$C_{PR}(s) = k_p + k_r \frac{2\omega_C s}{s^2 + 2\omega_C s + \omega_0^2} \tag{12}$$

is often implemented for the closed-loop control of systems with sinusoidal behavior. Due to its performance and simple implementation, it is often used in power electronics for single-phase alternating currents/volts control [16]. It is also possible to obtain a certain approximation of repetitive control by using several such controllers with different specific frequencies in the parallel structure. It can be obtained as

$$Q(s) = 1, \; R(s) = \frac{2\omega_C s}{s^2 + 2\omega_C s + \omega_0^2}, \; F(s) = 0. \tag{13}$$

- **Lead/Lag controller**: Controller, in the form

$$C_{LL}(s) = k \cdot \frac{T_1 s + 1}{T_2 s + 1} = k_q + k_r \frac{s}{T_2 s + 1}, \tag{14}$$

can be obtained as

$$Q(s) = 1, \quad R(s) = \frac{s}{T_2 s + 1}, \quad F(s) = 0. \tag{15}$$

- **BandPass controller**: A second-order controller can be obtained as

$$Q(s) = 1, \quad R(s) = \frac{\tau_H s}{(\tau_L s + 1)(\tau_H s + 1)}, \quad F(s) = 0. \tag{16}$$

2.3 H_∞ design specifications

Consider that

$$H(s, \mathbf{k}) = W(s)S_*(s, \mathbf{k}), \tag{17}$$

where $S_*(s, \mathbf{k})$ is an arbitrary closed-loop sensitivity function (2-5) and $W(s)$ is a stable weighting function. Closed-loop design requirements can now be expressed in a unified form

$$|H(j\omega, \mathbf{k})| \leq \gamma, \qquad \forall \omega \in \langle 0, +\infty \rangle \tag{18}$$

or equivalently

$$\|H(s, \mathbf{k})\|_\infty \leq \gamma, \tag{19}$$

where $\|H\|_\infty \triangleq \sup_\omega |H(j\omega)|$ is called H_∞-norm.

3. Basic Design Problem

The elementary problem of designing the fixed-structure controllers is to determine all stabilizing controllers such that the closed-loop system is internally stable and the performance/robustness criterion (19) holds. We suppose the stable rational function $H(s, \mathbf{k}) \in RH_\infty$ equals to

$$H(s, \mathbf{k}) = \frac{H_n(s, \mathbf{k})}{H_d(s, \mathbf{k})}, \tag{20}$$

where $H_n(s,\mathbf{k})$ and $H_d(s,\mathbf{k})$ are coprime polynomials with real coefficients. Similarly, we can rewrite the controller (1) to

$$C(s,\mathbf{k}) = k_q\frac{Q_n(s)}{Q_d(s)} + k_r\frac{R_n(s)}{R_d(s)} + \frac{F_n(s)}{F_d(s)}. \tag{21}$$

Let $\mathcal{K}$ is the set of all controller parameters $\mathbf{k} = [k_r, k_q]$ satisfying the performance/robustness criterion (19).

$$\mathcal{K} = \Big\{\mathbf{k}\in\mathbb{R}^2, \Big|H_n(j\omega,\mathbf{k})\Big| \le \gamma\cdot\Big|H_d(j\omega,\mathbf{k})\Big|, \omega\in[0,\infty)\Big\}. \tag{22}$$

We will hereafter call this set the H_∞ **region** and the controller $C(s,\mathbf{k})$ for $\mathbf{k}\in\mathcal{K}$ the H_∞ **controller**. We first find a set of certain curves that contain the boundary $\delta\mathcal{K}$ of the H_∞ region $\mathcal{K}$ as its subset.

Theorem 1. [7] *The boundary of the set $\mathcal{K}$ is contained in the solution of the systems*

$$\begin{cases} H_n(j\omega,\mathbf{k}) = 0, & (23a)\\ H_d(j\omega,\mathbf{k}) = 0, & (23b)\end{cases}$$

$$\begin{cases} |H(j\omega,\mathbf{k})|^2 = \gamma^2, & (24a)\\ \dfrac{\partial|H(j\omega,\mathbf{k})|^2}{\partial\omega} = 0, & (24b)\end{cases}$$

for $\omega\in\langle 0,+\infty)$ and three equations

$$|H(0,\mathbf{k})| = \gamma, \tag{25}$$

$$|H(j\infty,\mathbf{k})| = \gamma, \tag{26}$$

$$h_d(\mathbf{k}) = 0, \tag{27}$$

where h_d is the coefficient at the higher order of a polynom $H_d(s,k)$.

An analysis of the **Theorem 1** systems allows the derivation of an analytical method for determining the boundary of H_∞ region. The following statements are given only for the case of the weighted sensitivity function (3). However, they can be extended to other cases by the Gröbner bases technique.

Let us consider the transfer function of the system $P(s)$ and the weighting function $W(s)$ in the rational coprime form

$$P(s) = \frac{P_n(s)}{P_d(s)} \tag{28}$$

and

$$W(s) = \frac{W_n(s)}{W_d(s)}, \tag{29}$$

respectively. The controller structure is intended in the affine form (21). For the case of $H(s,\mathbf{k}) = W(s)S(s,\mathbf{k})$ then holds that

$$H(s,\mathbf{k}) = \frac{W_n(s)Q_d(s)R_d(s)F_d(s)P_d(s)}{H_d(s,\mathbf{k})}, \tag{30}$$

where $H_d(s,\mathbf{k}) = W_d(s)\big(F_d(s)P_n(s)Q_d(s)R_n(s)k_r + F_d(s)P_n(s)Q_n(s)R_d(s)k_q + Q_d(s)R_d(s)F_d(s)P_d(s) + F_n(s)P_n(s)Q_d(s)R_d(s)\big)$.

3.1 Analysis of the system (23)

Lemma 1. *$H_n(j\tilde\omega,\boldsymbol{k}) = 0$, $\tilde\omega\in\mathbb{R}$, if and only if one of the following two conditions holds:*

(i) At least one of the transfer functions $Q(s)$, $R(s)$, $F(s)$, and $P(s)$ has a pole $j\tilde\omega$, $\tilde\omega\in\mathbb{R}$ on the imaginary axis of the complex plane.

(ii) The weighting function $W(s)$ has zero $j\tilde\omega$, $\tilde\omega\in\mathbb{R}$ on the imaginary axis of the complex plane.

Proof. The proof follows directly from the relation (30). □

Lemma 2. *Let $\tilde\omega\in\mathbb{R}$ satisfies **Lemma 1** and assume that $W_d(j\tilde\omega)\neq 0$ then the system (23) has a solution iff there exists $\tilde{\boldsymbol{k}} = [\tilde k_r, \tilde k_q]$ such that $H_d(j\tilde\omega,\tilde{\boldsymbol{k}}) = 0$ or equivalently iff at least one of the following conditions is true*

$$\begin{aligned}
&(i) & \tilde k_q\cdot F_d(j\tilde\omega)P_n(j\tilde\omega)Q_n(j\tilde\omega)R_d(j\tilde\omega) &= 0,\\
&(ii) & \tilde k_r\cdot F_d(j\tilde\omega)P_n(j\tilde\omega)Q_d(j\tilde\omega)R_n(j\tilde\omega) &= 0,\\
&(iii) & F_n(j\tilde\omega)P_n(j\tilde\omega)Q_d(j\tilde\omega)R_d(j\tilde\omega) &= 0,\\
&(iv) & \tilde k_q\cdot F_d(j\tilde\omega)P_n(j\tilde\omega)Q_n(j\tilde\omega)R_d(j\tilde\omega) &+\\
&& +\ \tilde k_r\cdot F_d(j\tilde\omega)P_n(j\tilde\omega)Q_d(j\tilde\omega)R_n(j\tilde\omega) &+\\
&& +\ F_n(j\tilde\omega)P_n(j\tilde\omega)Q_d(j\tilde\omega)R_d(j\tilde\omega) &= 0,\\
&(v) & H_d(j\tilde\omega,\tilde{\boldsymbol{k}})/W_d(j\tilde\omega) &= 0.
\end{aligned}$$

Proof. If $\tilde\omega\in\mathbb{R}$ satisfies **Lemma 1** then it holds that $H_n(j\tilde\omega,\mathbf{k}) = 0$. Now, the system (23) has the solution iff there exists $\tilde{\mathbf{k}}$ such that $H_d(j\tilde\omega,\tilde{\mathbf{k}}) = 0$. The rest of the proof follows from (30) and the fact that

$$H_n(j\tilde\omega,\mathbf{k}) = 0 \;\Leftrightarrow\; \big(\,Q_d(j\tilde\omega) = 0 \;\vee\; R_d(j\tilde\omega) = 0 \;\vee\; F_d(j\tilde\omega) = 0 \;\vee\; P_d(j\tilde\omega) = 0 \;\vee\; W_n(j\tilde\omega) = 0\,\big). \tag{31}$$

□

If we exclude the singular case (iii), when $H(s,\mathbf{k})$ does not depend on the parameter $\mathbf{k}$ at all, we obtain in all other cases that the solution of the system (23) corresponds to a straight line in the parametric plane $k_r - k_q$. In case (i), it is the k_r axis. In case (ii), it is the k_q axis. In cases (iv) and (v), it is the general straight line in the $k_r - k_q$ parametric plane.

3.2 Analysis of the system (24)

Lemma 3. *Assume that (23b) does not hold, then the equation (24a) can be expressed equivalently in the form*

$$p_1(\omega, \boldsymbol{k}) = 0, \tag{32}$$

where $p_1(\omega, \boldsymbol{k})$ is a second-order polynomial with real coefficients in the variables k_r and k_q.

Proof. From (17), (24a) and (30), it follows that

$$\left|H(j\omega, \mathbf{k})\right|^2 = \frac{H_n(j\omega)H_n(-j\omega)}{H_d(j\omega, \mathbf{k})H_d(-j\omega, \mathbf{k})} = \gamma^2. \tag{33}$$

Now, using appropriate notation, we obtain

$$\left|H(j\omega, \mathbf{k})\right|^2 = \frac{\vartheta_n(\omega)}{\varrho_d(\omega, \mathbf{k})} = \gamma^2, \tag{34}$$

where $\vartheta_n(\omega)$ is a polynomial in ω and $\varrho_d(\omega, \mathbf{k}) \neq 0$ by assumption. The equation (34) is equivalent with

$$\vartheta_n(\omega) - \gamma^2 \varrho_d(\omega, \mathbf{k}) = 0, \tag{35}$$

where the left side of (35) is clearly the required second-order polynomial $p_1(\omega, \mathbf{k})$ from the statement of **Lemma 3**. □

Lemma 4. *Assume that (23b) does not hold, then the equation (24b) can be expressed equivalently in the form*

$$p_2(\omega, \boldsymbol{k}) = 0, \tag{36}$$

where $p_2(\omega, \boldsymbol{k})$ is a second-order polynomial with real coefficients in the variables k_r a k_q.

Proof. From (34), it follows that

$$\left|H(j\omega, \mathbf{k})\right|^2 = \frac{\vartheta_n(\omega)}{\varrho_d(\omega, \mathbf{k})}. \tag{37}$$

By differentiating with respect to ω, we obtain

$$\frac{d}{d\omega}\left|H(\omega, \mathbf{k})\right|^2 = \frac{\frac{d}{d\omega}\vartheta_n(\omega)\varrho_d(\omega, \mathbf{k}) - \vartheta_n(\omega)\frac{d}{d\omega}\varrho_d(\omega, \mathbf{k})}{\varrho_d{}^2(\omega, \mathbf{k})}. \tag{38}$$

Since $\varrho_d(\omega, \mathbf{k}) \neq 0$ by assuption, the equation (24b) is equivalent to

$$\frac{d}{d\omega}\vartheta_n(\omega)\varrho_d(\omega, \mathbf{k}) - \vartheta_n(\omega)\frac{d}{d\omega}\varrho_d(\omega, \mathbf{k}) = 0, \tag{39}$$

where the left side of (39) is clearly the required second-order polynomial $p_2(\omega, \mathbf{k})$ from the statement of **Lemma 4**. □

The solution of the system (24) can be determined analytically by converting (32) and (36) to an algebraic equation of the fourth degree with one unknown (see Appendix A).

3.3 Analysis of the equations (25), (26) and (27)

The equation (25) and (26) are equivalent to the equations

$$p_1(0, \mathbf{k}) = 0 \quad \text{and} \quad \lim_{\omega \to \infty} p_1(\omega, \mathbf{k}) = 0,$$

where $p_1(\omega, \mathbf{k})$ is the second-order polynomial from **Lemma 3**. Therefore, the solutions of both these equations are a conic section in the parametric plane $k_r - k_q$ [11].

Finally, the left side of the equation (27) is at most a first-order polynomial with real coefficients in variables k_r and k_q. Therefore, the solution of this equation is the straight line or the empty set in the parametric plane $k_r - k_q$.

3.4 Sketch of H_∞ region isolation algorithm

Step 1 According to **Theorem 1**, we find all points in the parametric plane of the controller $C(s, \mathbf{k})$ suspected of being the boundary $\delta\mathcal{K}$. These points lie on a finite number of curves defined by the equations (23-27) in **Theorem 1**. We denote the set of all these curves by the symbol $\mathcal{B}$.

Step 2 From the curves of the set $\mathcal{B}$, found in step 1, we select those of their parts that meet H_∞ specification (19) of the design problem and the condition of internal stability. We denote the set of selected sections with the symbol $\mathcal{B}^*$.

Step 3 The curve segments of the set $\mathcal{B}^*$, found in step 2, form the boundary of one or several regions in the parametric plane of the controller. The regions obtained in this way can be bounded or unbounded. The union of the regions obtained in this way determines the searched set $\mathcal{K}$ of all H_∞ controllers meeting the elementary H_∞ specification (19).

4. Application Examples

In this section, we will introduce the software tool **PID Hinf Designer** and one practical example that demonstrates the applicability potential of the design method.

4.1 PID Hinf Designer

This MATLAB-based software is an advanced interactive tool for analyzing, designing, and tuning two-parameter-constrained affine controllers. The tool was developed and is distributed by REX Controls company, which is in close collaboration with the Faculty of Applied Sciences and NTIS - European Centre of Excellence. The application enables not only the general form of the controller[1] (1) but also its special cases (see Section 2.2). The tool can also be used for many more complicated design problems, such as cascade control or repetitive control (see [5]). In addition, the proposed controller can be expanded with a fixed serial or parallel compensator. In the case of serial connection, this compensator can be used to specify the design requirements further. In the case of parallel connection, we get a path to an iterative modification and improvement of the obtained solution. The tool is also adapted for so-called model sets, a form of description of the process

[1] This controller is labelled as QRF in the PID Hinf Designer.

provided by PIDMA autotuner [12]. Alternatively, obtaining a process model from experimental input-output data is also supported. The software is available at *www.pidlab.com*

4.2 Example [16]: Grid Connected Photovoltaic Inverter

The task is to find a PR current controller (12) with additional PR selective harmonic compensators for a single phase 3 kW Grid-Connected Photovoltaic Inverter system, which is connected to the grid through an LCL filter $G_f(s)$. This filter is extended by the processing delay $G_d(s)$ of the microcontroller. The design is therefore made for the system $P(s) = G_d(s)G_f(s)$.

$$P(s) = \frac{1}{1\times 10^{-4}s+1}\cdot \frac{s^2+1.143\times 10^4 s+1.587\times 10^8}{0.0012s^3+21.71s^2+3.016\times 10^5 s} \tag{40}$$

The whole design process is carried out in four steps. The first step deals with the fundamental PR controller, whose purpose is to track a current sinusoidal reference waveform.

Step 1: We consider a PR controller (12). The fundamental resonant frequency is 50 Hz, i.e. $\omega_0 = 314.159$ rad·s^{-1}, and the resonant cut-off frequency is set as $\omega_c = 0.5$ rad·s^{-1}. H_∞ constraint is apply on (3) according to (19) with $\gamma = 1.2$. Based on these specifications, the boundary of the H_∞ region is calculated in the parametric plane $k_r - k_p$, shown in Fig. 3. The specific solution $k_r = 3187.3$ and $k_p = 17.47$ is then selected from this region.

In the following steps, we will gradually improve the properties of the controller from *Step 1* (see Section 2.2). Additional PR harmonic compensators, applied for the 3rd, 5th and 7th harmonics, reduce or even eliminate these particular harmonic frequencies in the output current. These harmonic frequencies can result due to the converter's non-linearities, or they can be already present in the grid.

Step 2: We consider a general affine controller (1) with transfer functions $Q(s)$ and $R(s)$ for the PR controller. The $F(s)$ function is equal to the "*Step 1*" controller. The resonant frequency of the 3rd harmonic is 150 Hz, i.e. $\omega_0 = 942.478$ rad·s^{-1}, and the resonant cut-off frequency is $\omega_c = 1.5$ rad·s^{-1}. H_∞ constraint is again select for (3) with $\gamma = 1.2$. The boundary of the H_∞ region is then in Fig. 3. The specific solution is $k_r = 566.43$ and $k_p = 1.7215$.

Step 3: In view of the previous step, the $F(s)$ function is equal to the sum of "*Step 1*" and "*Step 2*" controllers. The resonant frequency of the 5th harmonic is 250 Hz, i.e. $\omega_0 = 1570.796$ rad·s^{-1}, and the resonant cut-off frequency is $\omega_c = 2.5$ rad·s^{-1}. H_∞ constraint is select for (3) with $\gamma = 1.21$. The boundary of the H_∞ region is then in Fig. 4. The specific solution is $k_r = 507.045$ and $k_p = 0.43817$.

Step 4: Here, the function $F(s)$ is already equal to the sum of all previous solutions. The resonant frequency of the 7th harmonic is 350 Hz, i.e. $\omega_0 = 2199.115$ rad·s^{-1}, and the resonant cut-off frequency is $\omega_c = 3.5$ rad·s^{-1}. H_∞ constraint is select for (3) with $\gamma = 1.215$. The boundary of the H_∞ region is then in Fig. 4. The specific solution is $k_r = 330.7$ and $k_p = 0.917$.

The transfer function of the complete controller structure is shown in (41).

$$\begin{aligned} C(s) = &\left(17.47 + 3187.3\frac{s}{s^2+s+(314.159)^2}\right)+\\ +&\left(1.722+566.43\frac{3s}{s^2+3s+(942.478)^2}\right)+\\ +&\left(0.0438+507.045\frac{5s}{s^2+5s+(1570.796)^2}\right)+\\ +&\left(0.917+330.7\frac{7s}{s^2+7s+(2199.115)^2}\right) \end{aligned} \tag{41}$$

Figure 5 shows the sensitivity function (3) for the solution provided here and proposed in [16]. The step response of the closed loop can be compared for both solutions in Fig. 6. Figure 7 shows the control deviation of both solutions in case of tracking a reference 50 Hz sinusoidal signal. The higher harmonic frequencies rejection is displayed in Fig. 8.

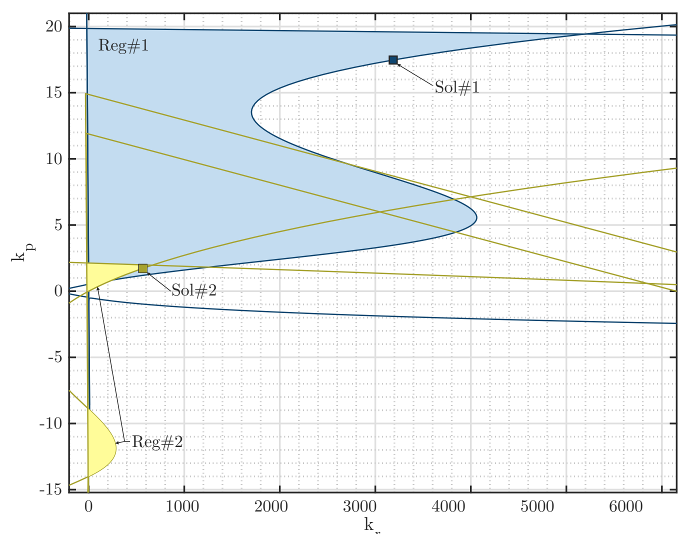

Figure 3. H_∞ region (■ Reg#1) with specific solution (■ Sol#1) for the design of the fundamental PR controller (*Step 1*). H_∞ region (■ Reg#2) with specific solution (■ Sol#2) for the design of 3rd harmonic compensator with additive fundamental PR controller (*Step 2*).

5. Conclusion

This paper introduces a new analytical method for the design of the H_∞ affine controller. This controller includes almost all fixed structure controllers commonly used in practice. By implementing the analytical method into a software tool, a

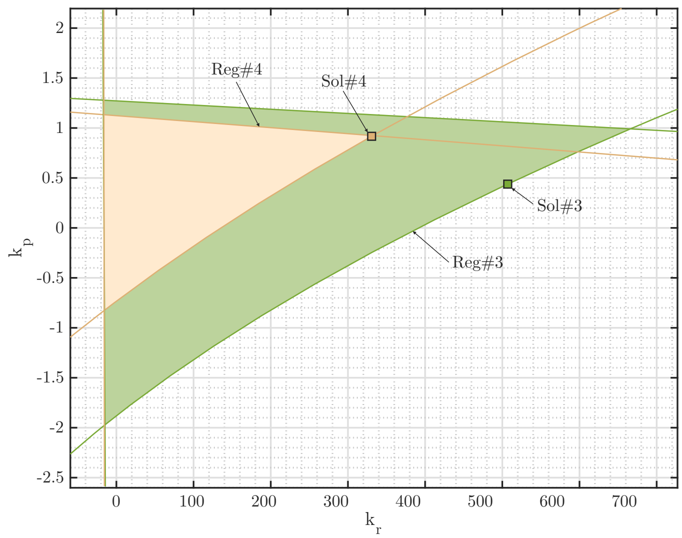

Figure 4. H_∞ region (Reg#3) with specific solution (Sol#3) for the design of 5th harmonic compensator with additive fundamental PR controller and 3rd harmonic compensator (*Step 3*). H_∞ region (Reg#4) with specific solution (Sol#4) for the design of 7th harmonic compensator with additive fundamental PR controller, 3rd and 5th harmonic compensators (*Step 4*).

powerful design instrument was obtained. The given example then presents its great application potential.

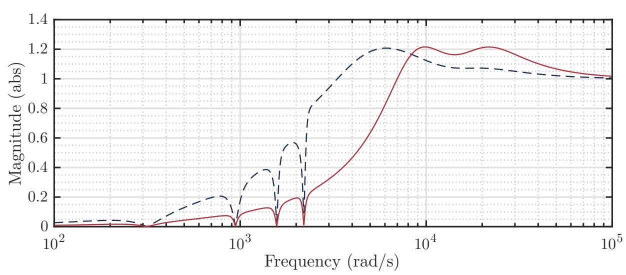

Figure 5. The sensitivity function (3) for the here designed solution (—) and the solution proposed in [16] (- -).

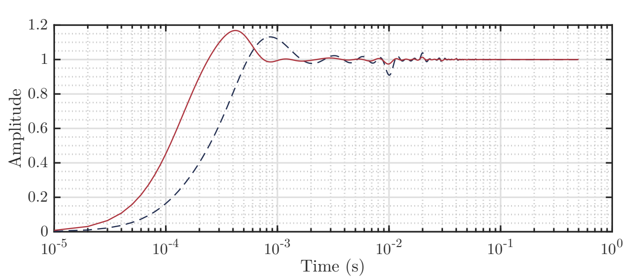

Figure 6. The step response of the closed-loop for the here designed solution (—) and the solution proposed in [16] (- -).

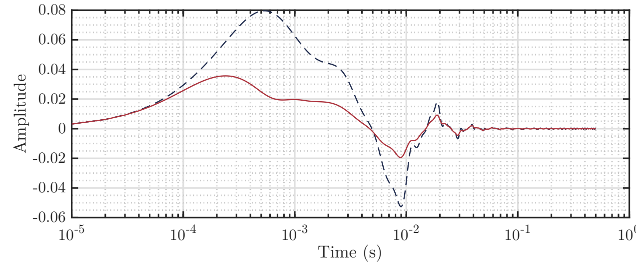

Figure 7. The control deviation of the here designed solution (—) and the solution proposed in [16] (- -) in case of tracking a reference 50 Hz sinusoidal signal.

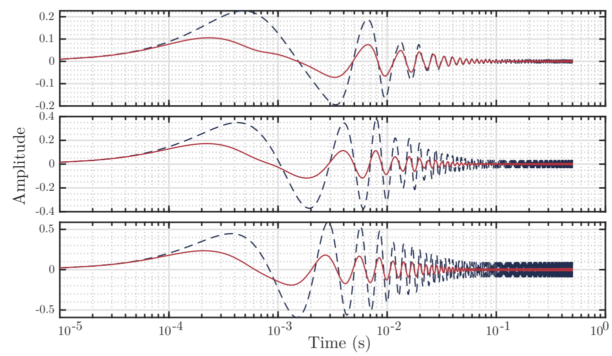

Figure 8. The comparison of the higher harmonic frequencies rejection by the here designed solution (—) and by the solution proposed in [16] (- -) in case of 150 Hz (a), 250 Hz (b) and 350 Hz (c) sinusoidal signal.

Appendix A.

Lemma 5. *The real solution of the system of equations*

$$\begin{aligned} ax^2 + by^2 + cxy + dx + ey + f &= 0, \\ gx^2 + hy^2 + mxy + nx + py + q &= 0, \end{aligned} \tag{42}$$

is determined as follows:

(i) $y_i, i = 1, \cdots, k, k \in \{2, 4\}$ *is a real root of the quartic equation*

$$C_a y^4 + C_b y^3 + C_c y^2 + C_d y + C_e = 0, \tag{43}$$

where $C_a = a^2h^2 - 2abgh + abm^2 - achm + b^2g^2 - bcgm + c^2gh$, $C_b = 2a^2hp - 2abgp + 2abmn - achn - acmp - adhm - 2aegh + aem^2 - bcgn - bdgm + 2beg^2 + c^2gp + 2cdgh - cegm$, $C_c = 2a^2hq + a^2p^2 - 2abgq + abn^2 - acmq - acnp - adhn - admp - 2aegp + 2aemn - 2afgh + afm^2 - bdgn + 2bfg^2 + c^2gq + 2cdgp - cegn - cfgm + d^2gh - degm + e^2g^2$, $C_d = 2a^2pq - acnq - admq - adnp - 2aegq + aen^2 - 2afgp + 2afmn + 2cdgq - cfgn + d^2gp - degn - dfgm + 2efg^2$ *and* $C_e = a^2q^2 - adnq - 2afgq + afn^2 + d^2gq - dfgn + f^2g^2$.

(ii) $x_i, i = 1, \cdots, k, k \in \{2, 4\}$ *is determined by relationship*

$$x_i \triangleq \frac{-y_i^2 ah + y_i^2 bg - y_i ap + y_i eg - aq + fg}{y_i am - y_i cg + an - dg}. \tag{44}$$

References

[1] H. Anai and S. Hara. A parameter space approach for fixed-order robust controller synthesis by symbolic computation. *IFAC Proceedings Volumes*, 2002.

[2] P. Apkarian and D. Noll. The $\mathcal{H}_\infty$ control problem is solved. *AerospaceLab Journal, ONERA*, 2017.

[3] F. Blanchini, A. Lepschy, S. Miani, and U. Viaro. Characterization of pid and lead/lag compensators satisfying given $\mathcal{H}_\infty$ specifications. *IEEE Transactions on Automatic Control*, pages 736–740, 2004.

[4] P. Dorato, W. Yang, and Ch. Abdallah. Robust multi-objective feedback design by quantifier elimination. *Journal of Symbolic Computation*, 1997.

[5] M. Goubej and M. Schlegel. Pi plus repetitive control design: H-infinity regions approach. *22nd International Conference on Process Control (PC19)*, 2019.

[6] E. Gryazina, B. Polyak, and A. Tremba. Design of the low-order controllers by the $\mathcal{H}_\infty$ criterion: A parametric approach. *Automation and Remote Control*, pages 456–466, 2007.

[7] E. Gryazina, B. Polyak, and A. Tremba. D-decomposition technique state-of-the-art. *Automation and Remote Control*, pages 1991–2026, 2008.

[8] E.N. Gryazina and B.T. Polyak. Stability regions in the parameter space: D-decomposition revisited. *Automatica*, 2006.

[9] M. T. Ho. Synthesis of $\mathcal{H}_\infty$ pid controllers: A parametric approach. *Automatica*, 39(6):1069–1075, 2003.

[10] L. H. Keel and S. P. Bhattacharyya. Robust, fragile, or optimal? *IEEE Transactions on Automatic Control*, 42(8):1098–1105, 1997.

[11] M. H. Protter and C. B. Morrey. *Analytic Geometry*. Addison-Wesley, 1966.

[12] M. Schlegel, P. Balda, and M. Štětina. Robust pid autotuner: Moment method. *Automatizace*, 2003. (in Czech).

[13] M. Schlegel and P. Medvecová. Design of pi controllers: $\mathcal{H}_\infty$ region approach. *IFAC-PapersOnLine*, pages 13–17, 2018.

[14] C. Spelta and E. N. Gryazina. Describing the h_∞ set in the controller parameters space. *2007 European Control Conference (ECC)*, 2007.

[15] M. T. Söylemez, N. Munro, and H. Baki. Fast calculation of stabilizing pid controllers. *Automatica*, 39, 2003.

[16] D. Zammit, C. Spiteri, M. Apap, and J. Licari. Design of pr current control with selective harmonic compensators using matlab. *Journal of Electrical Systems and Information Technology*, 2017.

[17] K. Zhou, J. C. Doyle, and K. Glover. *Robust and Optimal Control*. Upper Saddle River: Prentice hall, 1996.

[18] K. J. Åström, Hélène Panagopoulos, and T. Hägglund. Design of pi controllers based on non-convex optimization. *Automatica*, pages 585–601, 1998.